مجلهٔ بلورشناسی و کانی‌شناسی ایران، سال هشتم، شمارهٔ یک، بهار و تابستان ۱۳۷۹ از صفحهٔ ۸۳ تا ۱۰۰

پژوهشی

# اسپسارتین گارنت با ساختار ماکل نوری متقارن پیدا شده در یک پیه مونتیت کوارتز شیست در ناحیهٔ آسمی گاوا در نوار دگرگونی سانباگاوا، در شیکوکوی مرکزی ژاپن

**جواد ایزدیار**

*گروه زمین‌شناسی، دانشکده علوم، دانشگاه زنجان*

چکیده: گارنت با ساختار ماکل نوری متقارن در یک نمونه از پیه مونتیت شیستهای منطقه آسمی گاوا واقع در نوار دگرگونی سانباگاوا یافت شد. نوار دگرگونی در جنوب غربی ژاپن واقع شده و در اثر دگرگونی ناحیه‌ای فشار بالا در زمان کرتاسه تشکیل شده است. گارنت حاوی میانبارهای متعددی از پیه مونتیت، کوارتز، هماتیت، برونیت، تالک و آمفیبولهای سدیک می‌باشد. بخش عمده گارنت ($X_{Sps} = 0.85$) از اسپسارتین تشکیل شده است و منطقه بندی شیمیایی در آن دیده نمی‌شود. پیه مونتیت در زمینه و به صورت میانبارهای در گارنت و آلبیت دیده می‌شود و حاوی منطقه بندی شیمیایی مشخص نیست. معمولاً مرکز پیه مونتیت حاوی درصد کمتری $Fe^{3+}$ و درصد بیشتری $Mn^{3+}$ و Al است. گارنت از لحاظ نوری ناهمسانگرد بوده و در نورهای قطبی عمود بر هم از بخشهای متعددی تشکیل شده است که دارای طرحهای هشت‌وجهی، شش وجهی و چهار وجهی است. برای تعیین نحوه ایجاد طرحهای دیده شده از مدل رومبودودکا هدرال استفاده شد و نشان داد که بخشهای با اندیسهای میلری متقارن خواص نوری مشابهی را نشان می‌دهند. ارتباطات بافتی و توزیع کاتیونهای Al، $Fe^{3+}$ و $Mn^{3+}$ در بین گارنت، پیه مونتیت و برونیت نشان می‌دهد که تشکیل گارنت ناشی از واکنش میان مونتیت و برونیت بوده است.

**واژه‌های کلیدی**: *گارنتهای ناهمسانگرد نوری، پیه مونتیت شیست، نوار دگرگونی سانباگاوا، اسپسارتین، ساختار بخشی*

Iranian Journal of Crystallography and Mineralogy, Vol.8, No.1, Spring 1379/2000

# Optically sector-twinned spessartine garnet from a piemontite quartz schist in the Asemi-gawa area of the Sanbagawa metamorphic belt, central Shikoku, Japan

**Javad Izadyar**

*Department of Geology, Faculty of Science, Zanjan University, Zanjan, Iran.*

**Keywords:** *Optically anisotropic garnet, Piemontite schist, Sanbagawa metamorphic belt, Sector structure, Spessartine garnet*

**Abstract** : Optically sector - twinned garnet was found in a piemontite quartz schist in the Asemi-gawa area from the Sanbagawa metamorphic belt. The Sanbagawa metamorphic belt was formed during a regional Cretaceous intermediate high pressure type of metamorphism which is present through Southwest Japan. The garnet contains abundant inclusions of piemontite, quartz, hematite, braunite, talc and sodic amphibole. It is almost homogenous spessartine garnet ($X_{Sps}$ = 0.85). Piemontite occurs both in matrix and as inclusion in garnet and albite and it usually shows distinct zonation in which core of the grain contains lower $Fe^{3+}$ and higher $Mn^{3+}$ - and Al-contents than those of the rim. The garnet is anisotropic and composed of several parts or sectors visible in crossed polars. They show different patterns such as octahedral, hexahedral and tetrahedral in which optical orientation and extinction position are roughly symmetrical. A rhombododecahedral model garnet was used to interpret the geometry of the optically sector structure and show that sectors with symmetrical Miller's indices have similar optical properties. Textural relation and systematic partitioning of $Mn^{3+}$ , $Fe^{3+}$ and Al among garnet, piemontite and braunite indicate that garnet formation is due to the piemontite and braunite reaction.

## Introduction

Sector structures are relatively common in metamorphic garnets which two kinds of them are known; first one is the textural sector structure in which each sector is recognized through inclusion geometry [1] and second one is the chemical or compositional sector structure in which each sector can be distinguished by different chemical composition [2, 3]. These two types have been also reported from Japanese metamorphic rocks both in low P/T metamorphic belts such as Abukuma [4, 5] and Higo [6] and in high pressure metamorphic complex, the Sanbagawa belt. Formation of sector structure has been attributed to rapid growth under disequilibrium and supersaturated conditions [2, 3].

On the other hand, optically non-cubic garnets showing birefringence have been reported by many mineralogists and petrologists [7]. Birefringence is especially common in grossular - andradite garnet from skarns, hydrothermal ore deposits and contact metamorphic rocks [8, 9]. The origin of birefringence in garnets has not been clarified but several hypotheses have been proposed to account for optical anisotropy: (1) strain arising from lattice mismatch at subgrain, composition or twin boundaries [10, 11]; (2) ordering of Al and $Fe^{3+}$ on the octahedral sites [12]; (3) ordering of Ca and $Fe^{2+}$ on the dodecahedral sites [9]; (4) presence of OH groups distributed in a noncubic manner [13].

The author found another kind of sector structure from the Sanbagawa metamorphic belt which is neither texturally nor chemically. In this kind, each sector can be identified by the optical properties thereby it is called optically sector structure. The purpose of the present contribution is to report such an occurrence of optically abnormal garnet and to discuss its geometry and forming reaction.

## Geological setting, Sample locality, Analytical procedure

The Sanbagawa metamorphic belt is a regional of Cretaceous intermediate high pressure type of metamorphism presents through Southwest Japan (Fig.1). A large proportion of the Sanbagawa

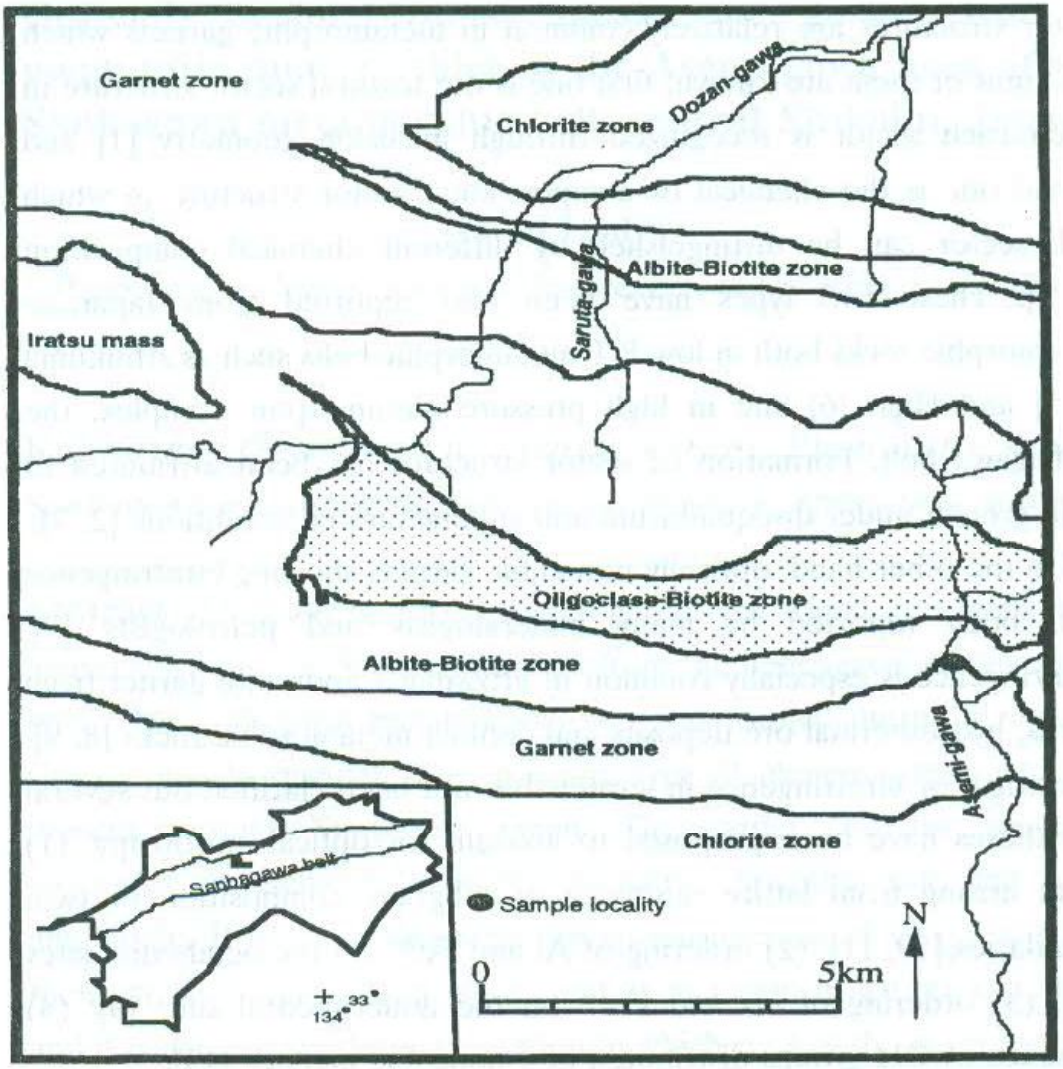


**Fig.1.** Metamorphic zonal map of the Sanbagawa metamorphic belt it central Shikoku (simplified from Higashino, 1990)[18] and sample locality.

metamorphic belt consists of pelite interbedded with varying amounts of oceanic materials and it is accompanied by ultramafic and mafic tectonic blocks in the highest grade part of central Shikoku [14]. Quartz schists, for example manganiferous and ferrogenous metachert that offers fascinating mineralogy are common in the schists [15]. In central Shikoku, the Sanbagawa metamorphic belt shows the widest distribution

and is divided into four mineral zones; chlorite, garnet, albite-biotite and oligoclase-biotite zones, based on the appearance of the index metamorphic minerals of the pelitic schists [15 - 17]. Its P-T range covers from 250-300°C and 5-6 kbars for the lower chlorite zone to the 610°C and 10-12 kbars to the oligoclase-biotite zone [15]. For further details of the geology and petrology of this area, the reader is referred to [15], [18] and [19]. Garnets occur in a piemontite quartz schist that was collected from the West bank of the Asemi-gawa, just north of the Kuwanokawa bridge (Fig. 1). It is located near the boundary between the garnet and albite-biotite zones and is probably the piemontite quartz schist layer from which Enami (1986) described ardennite [20].

Chemical analyses were done by a scanning electron microprobe (Hitachi S550) with a Kevex energy-dispersive X-ray analytical system using the correction subroutine of Magic V program of Kevex 7000 m system at Kyoto university. Working standards were pure metals for Mn, Cr and Ni, albite, wollastonite and orthoclase for Na, Ca and K, and finally oxides for Al, Fe, Mg, Ti. Details of the procedure follow Mori and Kanehira (1984) [21] and Hirajima and Banno (1991) [22]. Back scattered electron (BSE) images were obtained using ka GW-BSE detector system of the scanning electron microscope (Hitachi S530 and S550) at 20 kv and a beam current of about 1000 picoamperes. X-ray maps were collected by Kevex Advanced Image softwere.

## Sample petrography and mineral chemistry

The host Piemontite quartz schist shows compositional banding of the piemontite-rich and quartz-rich bands. The width of the piemontite, garnet, talc and hematite with subordinate amounts of quartz, phengite, albite and braunite. The quartz-rich band mostly contains quartz, phengite, albite, talc and chlorite with minor amounts of piemontite, garnet, hematite and braunite, and the width of these bands ranges from 1 to 2 mm.

Piemontite occurs both as separate grains in the matrix and as

inclusions in granet and albite. The following three end members; clinozoesite (Czo), pistacite (Ps) and piemontite (Pi) can explain the composition of piemontite. By using compositional and textural evidences, the author recognized two different generations of piemontites. Piemontite of the first generation that is referred to niemontite 1 usually forms large crystal that dominates the assemblage by its modal abundance. Piemontite of the second generation (piemontite 2) commonly occurs as narrow rim around piemontite 1. Piemontite 2 contains higher $Fe^{3+}$ and lower $Mn^{3+}$ and Al than piemontite 1 (comparing average composition of core $X_{Pi} = 0.26$, $X_{Ps} = 0.09$, $X_{Czo} = 0.65$ with the average composition of rim $X_{Pi} = 0.21$, $X_{Ps} = 0.19$, $X_{Czo} = 0.60$, $X_{Pi} = Mn^{3+}/Al+Mn^{3+} + Fe^{3+}$). Obviously piemontite 2 contains lower Ca in seven-to eigth-coordinated sites. In this case, some divalent Mn substitute for Ca. In most of the analyzed piemontites, deficits in the seven- to eight-coordinaed sites were seen in which some amounts of Sr or Pb could be present (Table 1).

Porphyroblasts of garnet occur in both piemontite and quartz-rich bands. Garnet in piemontite-rich bands is euhedral and its size ranges from 1 to 3 mm. This type of garnet is poikiloblastic, containing many inclusions of piemontite, quartz, hematite, braunite, talc and amphibole. Chemically, these garnets are Ca-Fe-bearing homogeneous spessartine with an average of $X_{Sps} = 0.85$, $X_{Grs} = 0.06$ and $X_{And} = 0.05$ (Table 2, Figs.3 and 4). The garnet in quartz rich bands includes only small amounts of hematite, piemontite and braunite. Such garnet is also Ca-Fe-bearing spessartine with $X_{Sps} = 0.84$, $X_{Grs} = 0.08$ and $X_{And} = 0.05$. In one sample, garnet locates within an albite porphyroblast in the quartz-rich band and it is chemically the same as those outside the albite (Table 2).

Talc occurs as tabular aggregate or as an intercalation with phengite or chlorite and is very close to the ideal Mg end-member.

Phengite is a major phyllosilicates in the studied samples and occurs

**Table 1.** Representative analyses of piemontite.

| Point No. | 5112 | 5212 | 1919 | 2019 | 332 | 132 |
|---|---|---|---|---|---|---|
| Core/Rim | Core | Rim | Core | Rim | Core | Rim |
| Wt% | | | | | | |
| SiO2 | 37.74 | 38.55 | 38.12 | 39.00 | 37.61 | 38.43 |
| TiO2 | 0.11 | 0.07 | 0.06 | 0.07 | 0.04 | 0.06 |
| Al2O3 | 20.55 | 19.07 | 20.59 | 19.51 | 20.30 | 18.81 |
| Fe2O3 | 2.90 | 9.78 | 3.82 | 9.34 | 6.11 | 9.10 |
| Mn2O3 | 14.58 | 11.75 | 13.28 | 12.70 | 11.35 | 12.34 |
| CaO | 22.99 | 19.81 | 22.48 | 18.98 | 23.04 | 19.64 |
| Total | 98.87 | 99.03 | 98.35 | 99.60 | 98.44 | 98.39 |
| No. of cations based on O=12.5 | | | | | | |
| Si | 3.01 | 3.07 | 3.04 | 3.08 | 3.01 | 3.05 |
| Ti | 0.01 | 0.01 | 0.01 | 0.01 | 0.00 | 0.01 |
| Al | 1.94 | 1.80 | 1.94 | 1.81 | 1.92 | 1.78 |
| Fe3+ | 0.18 | 0.58 | 0.24 | 0.56 | 0.37 | 0.55 |
| Mn3+ | 0.88 | 0.62 | 0.81 | 0.61 | 0.69 | 0.67 |
| Total | 3.01 | 3.01 | 3.00 | 2.99 | 2.98 | 3.01 |
| Ca | 1.96 | 1.69 | 1.93 | 1.60 | 1.98 | 1.69 |
| Mn2+ | - | 0.01 | - | 0.14 | - | 0.08 |
| Total | 1.96 | 1.70 | 1.93 | 1.74 | 1.98 | 1.77 |
| End members | | | | | | |
| Pi | 29.34 | 20.66 | 27.00 | 20.33 | 23.00 | 22.33 |
| Ps | 6.00 | 19.33 | 8.00 | 18.66 | 12.33 | 18.33 |
| Czo | 64.66 | 60.01 | 65.00 | 61.01 | 64.67 | 59.34 |

1-All of the Mn and Fe are considered as Mn2O3 and Fe2O3

2-Mn2+ and Mn3+ are computed based on structural formula

**Table 2.** Representative analyses of garnet in piemontite-rich and quartz-rich bands.

| | In piemontite_ rich band | | In quartz rich_ band | Enclosed in albite |
|---|---|---|---|---|
| Point No. | 27 | 43c | 130 | 150 |
| Wt% | | | | |
| SiO2 | 37.39 | 37.20 | 37.46 | 37.92 |
| TiO2 | 0.23 | 0.28 | 0.25 | - |
| Al2O3 | 19.58 | 19.01 | 19.62 | 19.71 |
| Fe2O3 | 1.74 | 1.96 | 1.73 | 1.93 |
| MnO | 36.92 | 36.28 | 35.71 | 36.24 |
| MgO | 0.71 | 0.42 | 0.57 | 0.63 |
| CaO | 4.08 | 3.97 | 4.47 | 4.36 |
| Total | 100.65 | 99.12 | 99.81 | 100.79 |
| NO. of cations based on O=12 oxygens | | | | |
| Si | 3.04 | 3.05 | 3.04 | 3.04 |
| Tl | 0.01 | 0.01 | 0.01 | - |
| Al | 1.86 | 1.84 | 1.87 | 1.87 |
| Fe2+ | - | - | - | - |
| Fe3+ | 0.09 | 0.12 | 0.10 | 0.12 |
| Mn | 2.55 | 2.52 | 2.46 | 2.47 |
| Mg | 0.08 | 0.05 | 0.07 | 0.08 |
| Ca | 0.34 | 0.34 | 0.38 | 0.37 |
| Total | 7.97 | 7.93 | 7.93 | 7.95 |
| End members | | | | |
| Sps | 85.86 | 86.60 | 84.50 | 84.50 |
| Pyr | 2.70 | 1.70 | 2.40 | 2.74 |
| Grs | 6.84 | 5.60 | 8.10 | 6.76 |
| And | 4.60 | 6.10 | 5.00 | 6.00 |
| Alm | 0.00 | 0.00 | 0.00 | 0.00 |

1- All of the Fe are considered as Fe2O3

2- Fe2+ and Fe3+ are computed based on structural formula

in the matrix and as an inclusion in albite porphyroblast. The average composition of phengite is:

$(K_{1.67}Na_{0.16})_{1.83}(Mg_{0.60}Fe^{3+}{}_{0.40}Al_{2.98})_{3.98}(Si_{6.70}Al_{1.34})_{8.08}O_{20}(OH)_4$ .

Chlorite is in contact with talc and phengite and its average composition is close to the ideal end-member of clinochlore.

Phlogopite can only found at the margin of the phengite. Its average chemical composition:

$(K_{1.84})(Mg_{5.47}Mn^{2+}{}_{0.13}Al_{0.13})_{5.73}(Si_{6.36}Al_{1.64})_{8.0}O_{20}(OH)_4$

The colorless amphibole presents as inclusion in albite and garnet

porphyroblasts and their chemical compositions correspond to crossite.

Porphyroblasts of albite commonly contain abundant inclusions of piemontite, hematite, phengite, talc, amphibole, quartz and rarely garnet.

Braunite (Br) occurs as aggregates of subhedral crystals that are intimately intergrown with quartz, or it is randomly interpersed as small particles among coarser grained main constiuents. Average chemical composition of braunite is:

$$(Ca_{0.03}Mn_{0.9}Mg_{0.01})_{0.94}(Mn^{3+}{}_{5.07}Fe^{3+}{}_{0.93})_6SiO_{12}$$

Hematite are in the matrix and as inclusions in albite and garnet and its average composition is: $(Fe_{1.90}Mn_{0.08}Ti_{0.01})_{1.99}O_3$

For further details on the chemical composition and petrological significance of the talc-phengite assemblage and on the chemical composition of piemontites and reaction relations between spessartine and piemontite, the interested reader is referred to [23] and [24]. The mineral abbreviations mainly follow Kretz (1983)[25].

## Optically sector-twinned garnet

Even though the garnets composed of several parts or sectors under crossed polars (Fig.2) but back-scattered electron imags and X-ray mapping (Figs.3 and 4) show that they are chemically identical. Under crossed polars, all sectors are anisotropic and their optical properties such as optical orientation and extinction position are roughly symmetrical with respect to the sector boundary. In figure 2 one octahedral section is shown and its sketch is drawn in figure 5A. Another sections such as tetrahedral and hexahedral were also seen which their sketches are drawn in figures 5B and C. In 180 degree clockwise rotation of microscope plane, starting from 140 location, extinction positions of the octahedral cross-section were shown in figure 6. In 140 location only sectors 3-7 and 1-5 are extinguished and with almost 40 degree rotation from 140, sectors 2-6 and 4-8 are now in the extinction positions. This procedure has symmetrically repeated with the

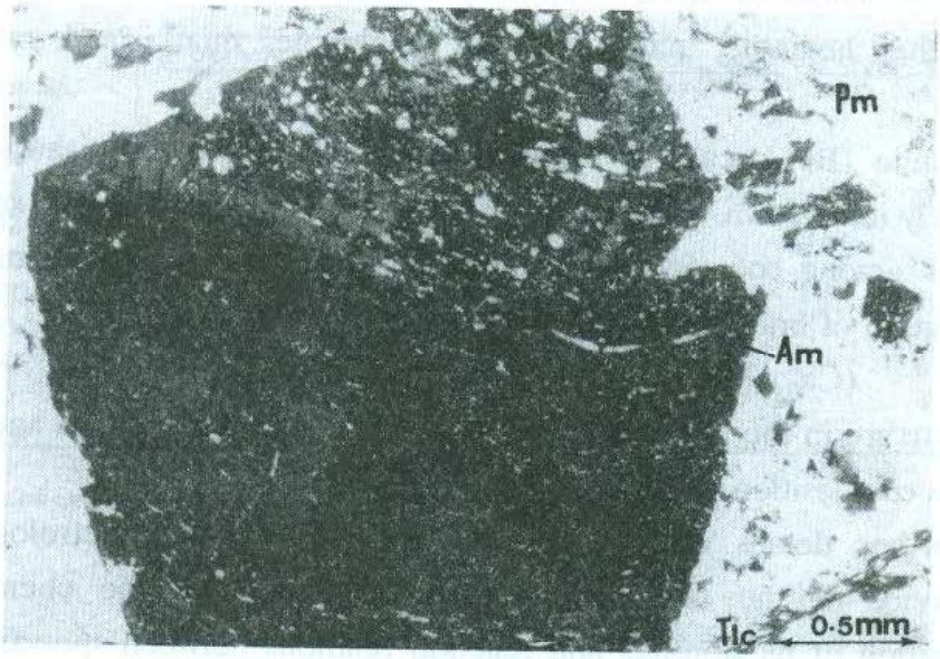


**Fig.2.** Photomicrograph of an octaghedral section of garnet under crossed polars.

continuation of the rotation. Gypsum ($\lambda$) plate was used to clarify optical orientations of the sectors. The results show that arrangements of na and nd differ for sectors with the same extinction positins. For example in 140 position, sectors 2-6 are in additional but sectors 4-8 are in subtraction positions which means that arrangements of na and nd differ for sectors 2-6 and 4-8. The same properties were seen for sectors 3-7 and 1-5 in location 100 which were in extinction in location 140. This procedure was examined for other types of cross-sections such as hexahedral and tetrahedral in which the same optical properties but with their own symmetries were concluded. One point should be noted that according to crystallographic definition, optical properties such as 2V and optical orientation must be symmetrical with respect to a twin plane. In discussed garnets, optical characters, which were possible to measure, are roughly symmetrical. Thus, these sectors are not twins in a strict

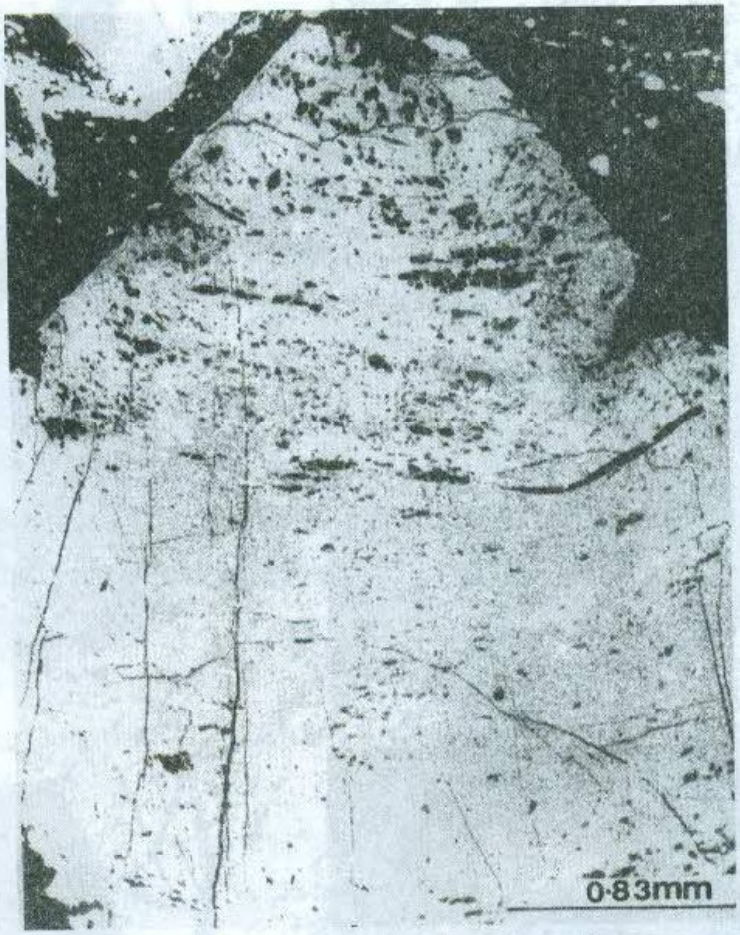


**Fig.3.** Back-scattered electron image of the octahedral section of garnet shown in figure 2.

crystallographic sense even though their symmetries are more than individual sectors. Therefore, the author prefers to use of the term optically sector-twinned garnet instance of zoning.

## Discussion

All of the observed patterns of the sector structures in garnet are possible to interpret in terms of cross sections of a rhombododecahedral crystal which proposed by Burton (1986) [26] and Yoshimura and Obata (1995) [6]. To find Miller's indices of different surfaces of rhombododecahedral, three Cartesian axes (X, Y, Z) are defined as

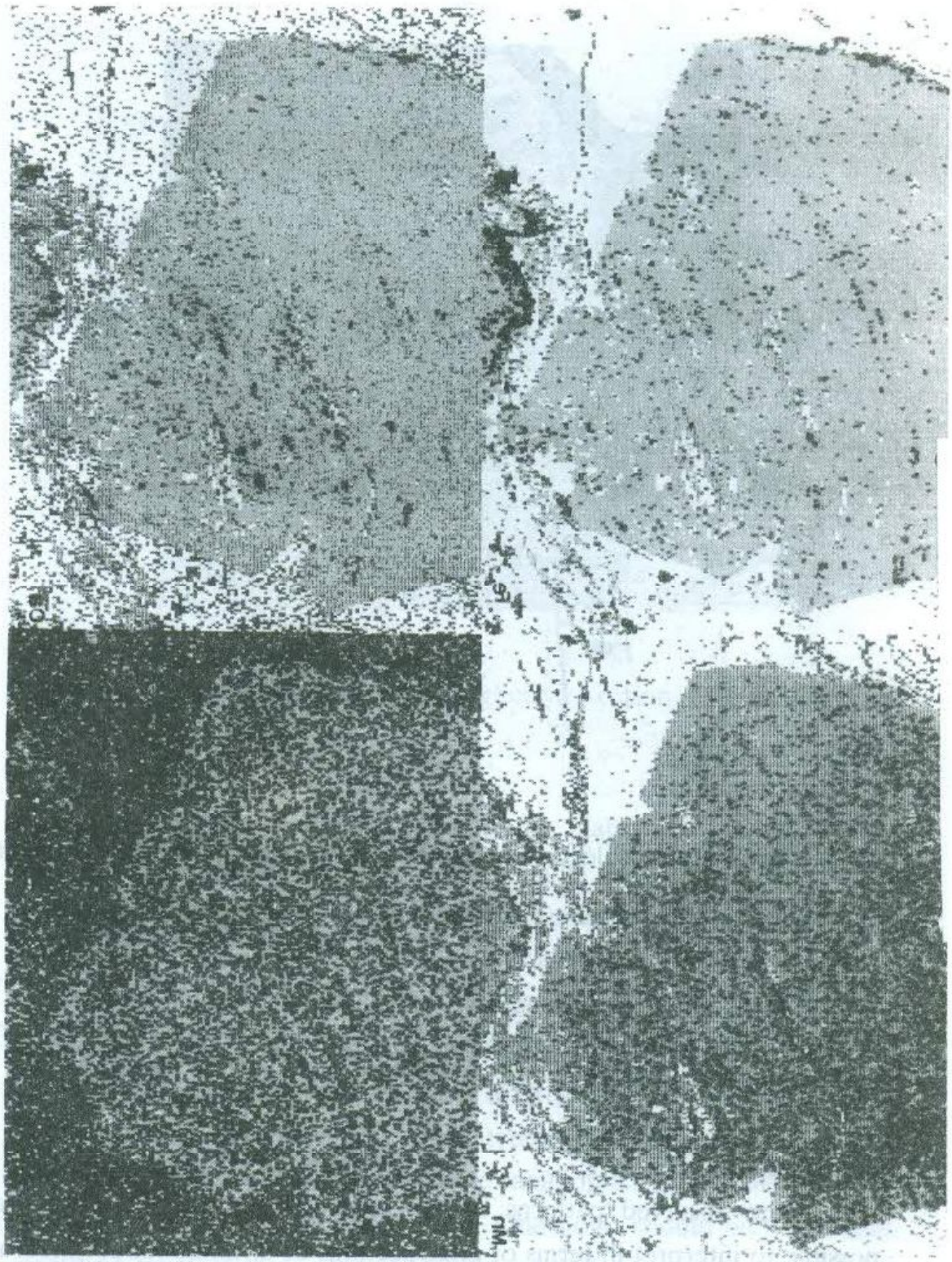


**Fig.4.** X-ray maps for Mn, Fe, Mg and Ca of the major part of theoctahedral section of garnet shown in figures 2 and 3.

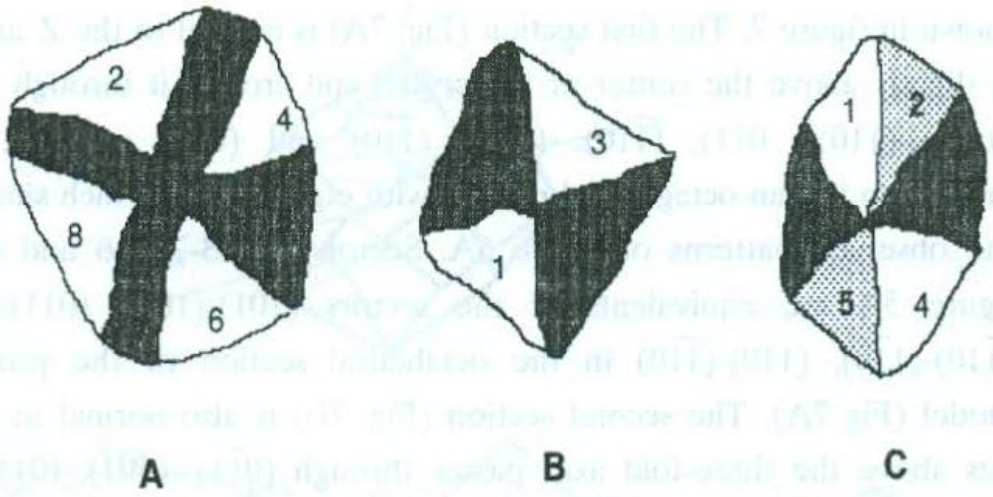


**Fig.5.** A, B and C are sketches of the observed optically anisotropic garnets under crossed polars.

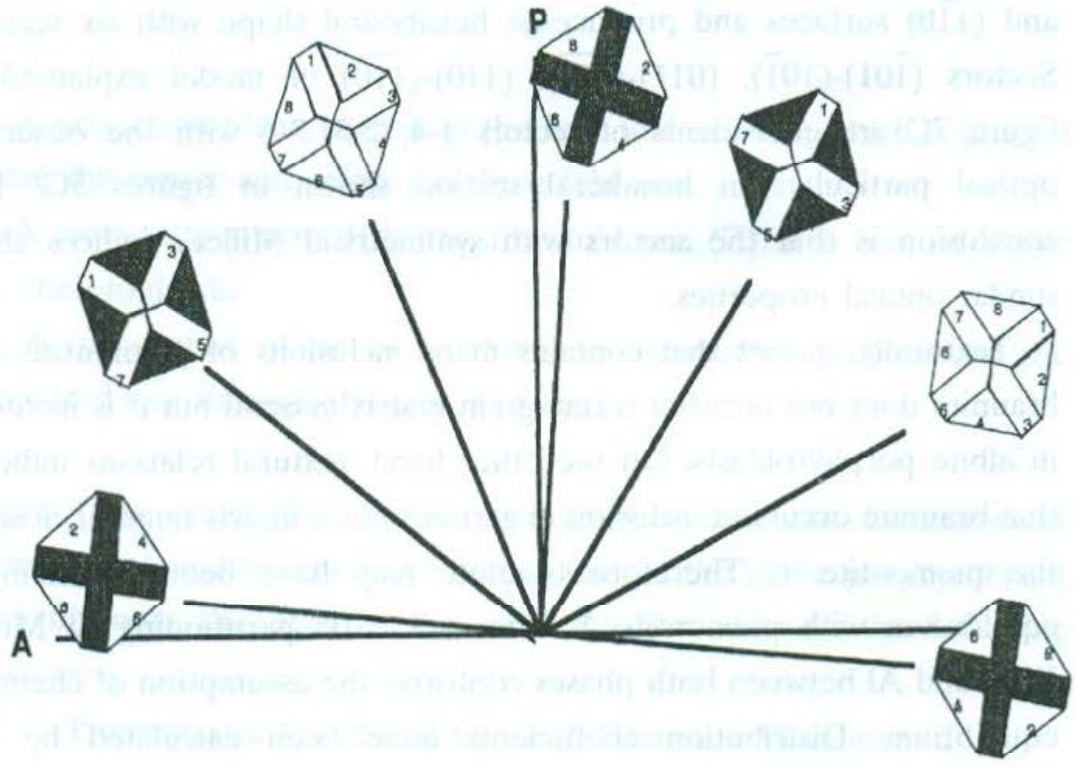


**Fig.6.** 180 degree clockwise rotation of an octahedral section in cross-polarized light. P and A are polarizer and analyzer directions.

shown in figure 7. The first section (Fig. 7A) is normal to the Z axis but is slightly above the center of the crystal and crosses it through $(1\bar{1}0)$, (101), (110),( 011), $(\bar{1}10)$, $(\bar{1}01)$, $(\bar{1}\bar{1}0)$ and $(0\bar{1}1)$ surfaces. This projection has an octaghedral outline with eight sectors which simulates the observed patterns of figure 5A. Sectors 1-5, 3-7, 2-6 and 4-8 in figure 5A are equivalents of the sectors $(\bar{1}01)$-(101), (011)-$(0\bar{1}1)$, $(\bar{1}10)$-$(1\bar{1}0)$, (110)-$(\bar{1}\bar{1}0)$ in the octahedral section of the proposed model (Fig 7A). The second section (Fig. 7B) is also normal to Z but lies above the three-fold axis, passes through $(0\bar{1}1)$, (101), (011) and $(\bar{1}01)$ surfaces, and has a lozenge shape with four sectors which can be correlated with the observed pattern of figure 5B. Sectors 1-3, 2-4 of the observed pattern in figure 5B correlate with sectors $(0\bar{1}1)$-(011), (101)-$(\bar{1}01)$ in the model (Fig. 7B). The third section (Fig. 7C), normal to the three-fold axis, passes through $(0\bar{1}\bar{1})$, $(10\bar{1})$, (110), (011), $(\bar{1}01)$ and $(\bar{1}\bar{1}0)$ surfaces and produces a hexahedral shape with six sectors. Sectors $(\bar{1}01)$-$(10\bar{1})$, (011)-$(0\bar{1}\bar{1})$, (110)-$(\bar{1}\bar{1}0)$ of model explained in figure 7C are equivalents of sectors 1-4, 2-5, 3-6 with the observed optical particulars in hexaheral section shown in figures 5C. The conclusion is that the sectors with symmetrical Miller's indices show similar optical properties.

Texturally, garnet that contains many inclusions of piemontite and braunite does not occur as a fine-grain matrix mineral but it is included in albite porphyroblasts. On the other hand, textural relations indicate that braunite occurs as inclusion in garnet or as a matrix mineral close to the piemontite 1. Therefore braunite may have been in chemical equilibrium with piemontite 1. The systematic partitioning of $Mn^{3+}$, $Fe^{3+}$ and Al between both phases conforms the assumption of chemical equilibrium. Distribution coefficients have been calculated by the following equations and show that relative to braunite, piemontite 1 is enriched in Al and $Fe^{3+}$ and depleted in $Mn^{3+}$.

$[KD_{(Al\text{-}Mn)} = (X_{Al}/X_{Mn})_{Pi}/(X_{Al}/X_{Mn})_{Br}; X_{Al} = Al/Al + Mn]$

$[KD_{(Fe\text{-}Mn)} = (X_{Fe}/X_{Mn})_{Pi}/(X_{Fe}/X_{Mn})_{Br}; X_{Mn} = Mn/Fe + Mn]$

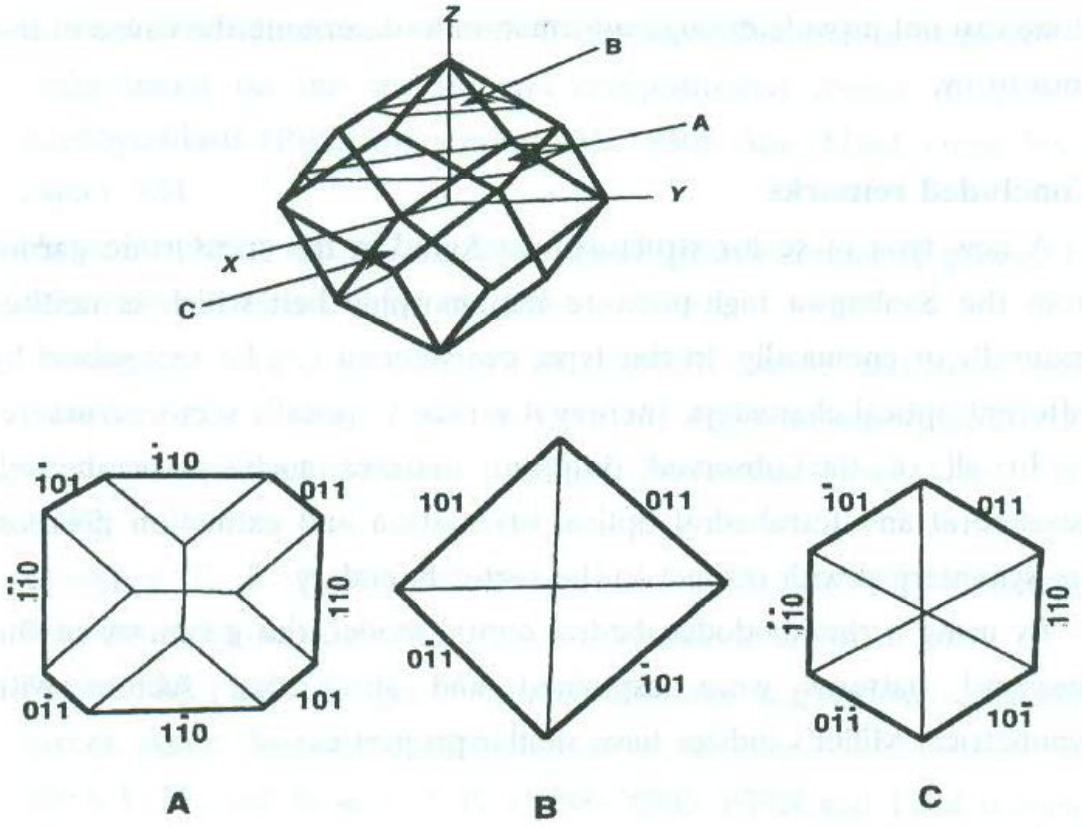


**Fig.7.**

A- A projection plane normal to the four-fold axis (Z) which is located above the center and below the three-fold axis.

B- A cross section normal to the four-fold axis (Z). It is located above the threefold axis.

C- A projection plane of a rhombododecahedron normal to the three-fold axis through the center of the crystal.

These facts imply that garnet was formed after the formation of piemontite 1 and braunite and before that of the albite porphyroblasts probably near the peak of the metamorphism through the following reaction.

Piemmontite 1 + Braunite === Garnet + Piemontite 2

The growth of garnet was probably done under disequilibrium condition which caused ordering of Ca and $Mn^{2+}$ on the dodecahedral site exposed on the growth surface, thereby reducing its symmetry from cubic even though it should be keep in mind that optical measurements

alone can not provide enough information to determine the cause of the anisotropy.

## Concluded remarks

1- A new type of sector structure was found in the spessartine garnet from the Sanbagwa high-pressure metamorphic belt which is neither texturally or chemically. In this type, every sector can be recognized by different optical characters, thereby it is called optically sector structure.
2- In all of the observed different patterns such as octahedral, hexahedral and tetrahedral optical orientation and extinction position are symmetrical with respect to the sector boundary.
3- By using a rhombododecahedral crystal model, the geometry of the observed patterns were explained and show that sectors with symmetrical Miller's indices have similar properties.

## Acknowledgment

During the preparation of the original draft in Kyoto university, I have benefited from the help of Emeritus Prof. S. Banno, Pro. M. Kitamura and Dr. T. Hirajima to whom my sincere thanks are due. The author would like to thank of helpful comments of ananymous reviewer. This study was generously supported by the Ministry of Education of Japan.

## References

1- Anderson, T. B. (1984) Inclusion patterns in zoned garnets from Magerfy, North Norway. Miner. Mag., 48, 21-6.
2- Kitamura, M., Wallis, S. R., and Hirajima T. (1993) Sector zoning and surface roughening of garnet in the Sanbagawa metamorphic rock. Proceeding of the Sixth Topical Meeting on Crystal Growth Mechanism, 215-220.
3- Shirahata, K., and Hirajima, T. (1995) Chemically sector-zoned garnet in Sanbagawa schists; its mode of occurrence and growth timing. J. Miner. Petro. Econ. Geol., 90, 69-79.

4- Kishi, S., and Hiroi, Y. (1987) P-T-t paths of Takanuki metamorphic rocks based on the texture and compositional zoning of garnet porphyroblasts (Preliminary note). Abt. 94th. Ann. Meet. Geol. Soc. Japan, 384.

5- Hiroi, Y. (1993) On the modification of growth zoning of garnet. J. Miner. Petro. Econ. Geol, 88, 189.

6- Yoshimura, Y., and Obata, M. (1995) Sector structure and compositoinal zoning of garnets from the Higo metamorphic rocks, west-central Kyushu, Japan. J. Miner. Petro. and Econ. Geol., 90, 80-92.

7- Meagher, E. P. (1980) Silicate garnets. In: Ribbe, P.H. (editor), Reviews in Mineralogy, Miner. Soc. America, 5, 25-58.

8- Akizuki, M. (1984) Origin of optical variations in grossular-andradite garnet. Amer. Miner., 69, 328-338.

9- Allen, F. M., and Buseck, P. R. (1988) XRD, FTIR and TEM studies of optically anisotropic garnets. Amer. Miner., 73, 568-584.

10- Chase, A. B. and Lefever, R. A. (1960) Birefringence of synthetic garnets. Amer. Miner., 45, 1126-1129.

11- Kitamura, K., and Komatsu, H. (1978) Optical anisotropy associated with growth striation of yttrium garnet. Kristallographie und Technic, 13, 811-816.

12- Takeuchi, Y., and Haga, N. (1982) The derivative structure of silicate garnets in grandite. Zeitschriftfur Kristallographie, 158, 53-99.

13- Rossman, G. R., and Aines, R. D. (1986) Spectroscopy of a birefringence grossular from Asbestos, Quebec, Canada. Amer. Minerl, 71, 779-780.

14- Wallis, S. R., Banno, S., and Radvance, M. (1992) Kinematics, structure and relationship to metamorphism of east-west flow in the Sanbagawa belt southwest, Japan. The Island Arc, 1, 176-185.

15- Banno, S., and Sakai, C. (1989) Geology and metamorphic evolutin of the Sanbagawa metamorphic belt, Japan. In: Dally, J.S., Cliff, R.A., Yardly, B.W.D. (eds) Evolution of metamorphic belts. Geol.

Soc. Spec. Pub., 43, 519-532.

16- Higashino, T. (1975) Biotite zone of Sanbagawa metamorphic terrain in the Siragayama area, central Shikoku, kJapan. J. Geol. Soc. Japan, 81, 653-670.

17- Enami, M. (1982) Oligoclase-biotite zone of the Sanbagawa metamorphic terrain in the Bessi district, central Shikoku, Japan. J. Geol. Soc. Japan, 88, 887-900.

18- Higashino, T. (1990) The higher grade metamorphic zonation of the Sanbagawa metamorphic belt in central Shikoku, Japan. J. Meta. Geol, 8, 413-423.

19- Wallis, S. R., and Banno S. (1990) The Sanbagawa belt-trends in research. J. Meta. Geol., 8, 393-399.

20- Enami, M. (1986) Ardennite in a quartz schist from the Asemi-gawa area in the Sanbagaw metamorphic terrain, central Shikoku, Japan. Miner, J., 13, 151-160.

21- Mori, K., and Kanehira, K. (1984) X-ray energy spectrometry for electron probe analysis. J. Geol. Soc. Japan, 90, 271-285.

22- Hirajima, T., and Banno, S. (1991) Electron-microprobe analysis of rock forming minerals with Kevex-delta IV (Quantum detector). Hitachi Scientific Instrument News, 34, 2-7.

23- Izadyar, J., Hirajima, T., and Nakamura, D. (2000) Talc-phengite-albite assemblge in piemontite-quartz schist of the Sandbagawa metamorphic belt, central Shikoku, Japan. The Island Arc, 9, 145-158.

24- Izadyar, J., (2000) Chemical composition of piemontites and reaction relations of piemontite and kspessartine in piemontite-quartz schists of central Shikoku, Sanbagawa metamorphic belt, Japan. Schweiz. Miner. Petro, Mitt., 80, 199-210.

25- Kretz, R. 1983. Symbols for rock-forming minerals. Amer. Miner., 68, 1023-52.

26- Burton, K. W. (1986) Garnet-quartz intergrowth in graphitic pelites: the role of the fluide phase. Miner. Mag., 50, 611-20.